

Exchange interactions in ZnMeO (Me=Mn,Fe,Co,Ni): Calculations using the frozen-magnon technique

L. M. Sandratskii and P. Bruno

Max-Planck Institut für Mikrostrukturphysik, D-06120 Halle, Germany

(Received 16 August 2005; revised manuscript received 20 October 2005; published 5 January 2006)

We report the density-functional-theory study of the electronic structure and exchange interactions in four diluted magnetic semiconductors (ZnMe)O, Me=Mn,Fe,Co,Ni. The calculations are performed for two impurity concentrations of 25% and 6.25%. For all systems the interatomic exchange interactions are short range with only the interaction between the nearest 3d impurities being sizable. For (ZnMn)O, the leading exchange interaction is antiferromagnetic for both impurity concentrations. In (ZnCo)O, the leading exchange interaction is ferromagnetic for high concentration and antiferromagnetic for low concentration. (ZnFe)O and (ZnNi)O are ferromagnetic for both concentrations. In all cases of the antiferromagnetic exchange interaction, the energy bands are either completely filled or empty. This reveals the connection between the presence of the charge carriers and ferromagnetism.

DOI: [10.1103/PhysRevB.73.045203](https://doi.org/10.1103/PhysRevB.73.045203)

PACS number(s): 75.50.Pp, 75.30.Et, 71.15.Mb

I. INTRODUCTION

The diluted magnetic semiconductors (DMS) are in the focus of the researches devoted to the design of materials for spintronic applications. The spintronic materials should combine such properties as high Curie temperature, high spin-polarization of the charge carriers, or the compatibility with the semiconductors used industrially. Since the prediction by Dietl *et al.*¹ of the Curie temperature of (ZnMn)O exceeding room temperature, the DMS on the ZnO basis attract strong research interest. However, despite many efforts the experimental situation remains highly controversial. For nominally the same systems the reports of the detection of high Curie temperature coexist with the reports that exclude an intrinsic ferromagnetism.^{2,3}

This unclear experimental situation enhances the role of the theoretical studies of the electronic properties of ZnMeO systems, where Me is a 3d impurity. Sato and Katayama-Yoshida⁴ considered ZnO doped with Mn, Fe, Co and Ni. The calculations have been performed with the Korringa-Kohn-Rostoker coherent potential approximation (KKR-CPA) method assuming random distribution of the 3d substitutional impurities on the Zn sites. The comparison of the total energies of the ferromagnetic and so-called disordered-local-moment (DLM) states has shown that the ferromagnetism is stable for Fe, Co, and Ni impurities and unstable for Mn impurity. Kulatov *et al.*⁵ and Risbud *et al.*⁶ used a supercell approach to calculate the electronic structure of ZnO doped with 3d impurities. Spaldin⁷ compared the energies of ferromagnetic and antiferromagnetic states of ZnO doped with Mn and Co for impurity concentrations of 6% and 12% and did not obtain a robust ferromagnetism. Park and Min⁸ extended the study of the electronic structure to the case of codoping with two different transition metals. In these theoretical studies the main attention was paid to the presence in the materials of charge carriers. (See a recent review³ for a detailed discussion of the experimental and theoretical situation.)

The purpose of the present work is a parameter-free calculation of the electronic structure and exchange interactions

for four DMS systems: (ZnMe)O, Me=Mn,Fe,Co,Ni. The calculations are performed for two strongly different impurity concentrations that allows the trends characteristic for high and low impurity contents to be revealed. We relate the features of the electronic structure to the properties of the exchange interactions.

II. CALCULATIONAL APPROACH AND RESULTS

A. Calculational scheme

The calculational scheme is discussed in Refs. 9–11 to which the reader is referred for more details. We use a supercell approach, choosing a fraction of the ZnO semiconductor crystal and replacing one of the Zn atoms by a 3d impurity. The larger the supercell, the lower the impurity concentration. We will discuss the results of the calculation for concentrations of 25% and 6.125% that corresponds to the use of the $1 \times 1 \times 2$ and $2 \times 2 \times 2$ supercells of the wurzite ZnO. The effects of the structural relaxation about the impurities were not taken into account.

For the calculation of the electronic structure and total energy, we use the augmented spherical waves (ASW) method.¹² The local-density approximation (LDA) to the energy functional is employed. The Zn 3d states were treated as core states to obtain better value of the semiconducting gap.¹³

To calculate the interatomic exchange interactions we use the frozen-magnon technique and map the total energy of the helical magnetic configurations onto a classical Heisenberg Hamiltonian,

$$H_{eff} = - \sum_{i \neq j} J_{ij} \mathbf{e}_i \cdot \mathbf{e}_j, \quad (1)$$

where J_{ij} is an exchange interaction between two Mn sites (i, j) and \mathbf{e}_i is the unit vector pointing in the direction of the magnetic moment at site i . The Curie temperature is estimated within the mean-field approximation

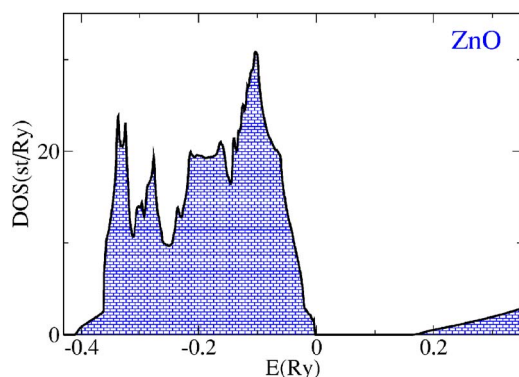


FIG. 1. (Color online) The density of states of ZnO.

$$k_B T_C^{MF} = \frac{2}{3} \sum_{j \neq 0} J_{0j}, \quad (2)$$

where J_{0j} are Heisenberg exchange parameters between two Mn sites $(0, j)$.

B. Density of states

We begin the discussion of the calculational results with the consideration of the electron density of states (DOS). In Fig. 1, we show the DOS of pure ZnO. The calculated gap is about 0.17 Ry. The valence-electron configurations of the substituting 3d atoms are Mn($3d^5 4s^2$), Fe($3d^6 4s^2$), Co($3d^7 4s^2$), and Ni($3d^8 4s^2$). The electron configuration of the substituted Zn atom is $4s^2$. According to the first Hund's rule, the minimum of the total energy of an isolated 3d atom corresponds to the occupation of the 3d orbitals that gives a highest spin moment. Therefore, in the case of a Mn atom, all five majority-spin 3d states are occupied while all minority-spin 3d states are empty. In the series Fe-Co-Ni the first Hund's rule predicts increasing partial occupation of the minority-spin 3d states.

Considering now the 3d atoms as impurities in ZnO we expect the formation of the electronic energy bands related to the Me(=Mn, Fe, Co, Ni) 3d states. The calculated electronic structures of the DMS (Figs. 2 and 3) are in agreement with the prediction of the Hund's rule: the energy bands associated with the majority-spin Me 3d states are occupied whereas the occupation of the minority-spin Me 3d states increases within the series of the 3d impurities Mn-Fe-Co-Ni.¹⁴ Indeed, the calculated electronic structures of the DMS are in agreement with this prediction (Figs. 2 and 3).

Let us first consider the DOS of the systems with impurity concentration of 25% (Fig. 2). We find the impurity bands lying, at least partly, within the semiconducting gap of ZnO. With increasing nuclear charge of the impurity, the impurity bands move to lower energy positions with respect to the semiconductor matrix. In (ZnMn)O, the majority-spin impurity band is completely filled and the minority-spin band is empty. Therefore (ZnMn)O has no charge carriers. For the Fe, Co, and Ni impurities, the minority-spin impurity band is partially filled.

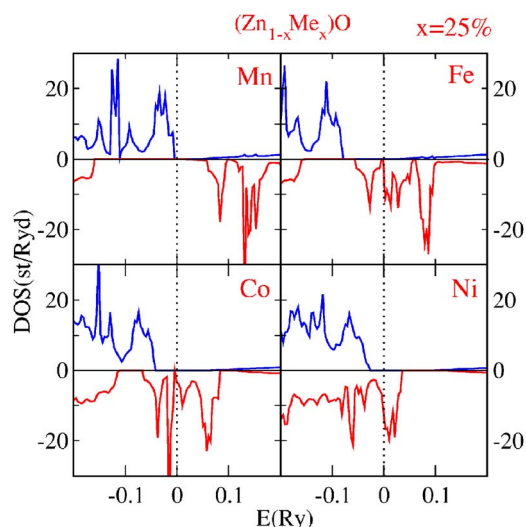


FIG. 2. (Color online) The density of states of (ZnMe)O with impurities Me=Mn, Fe, Co, Ni. The concentration of impurities is 25%.

In the case of impurity concentration of 6% (Fig. 3) the situation is qualitatively similar. An increased distance between the 3d atoms leads, however, to increased effective masses of the impurity-band states. The narrowing of the electron bands results in the energy separation of the e and t_2 minority-spin subbands. The splitting of the five-times degenerate atomic minority-spin 3d level into the e and t_2 subgroups is caused by the influence of the crystal environment. In the DMS with $x=25\%$, the energy bands are broader and, therefore, the energy separation of the e and t_2 subsystems does not take place. The filling of the minority-spin e subband begins in (ZnFe)O. In (ZnCo)O the e subband is completely filled and the t_2 subband is empty. As a result, (ZnCo)O at the impurity concentration of 6% has no charge carriers. In (ZnNi)O, the minority-spin t_2 subband is partially filled.

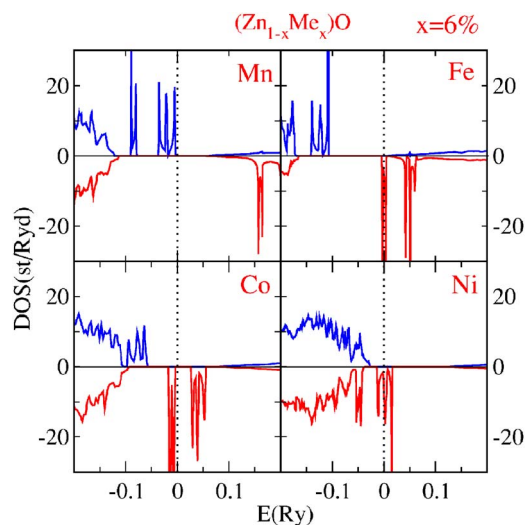


FIG. 3. (Color online) The density of states of (ZnMe)O with impurities Me=Mn, Fe, Co, Ni. The concentration of impurities is 6%.

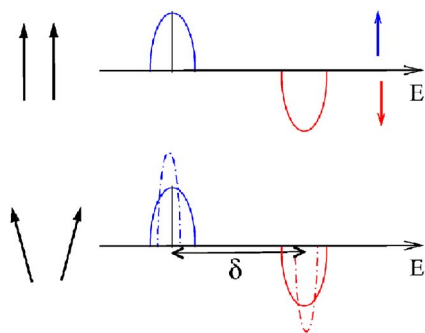


FIG. 4. (Color online) Schematic picture illustrating two types of the changes caused by the deviation of the atomic moments from the parallel directions. The upper panel shows a model spin-polarized DOS of a ferromagnet. The vertical line shows the position of the Fermi level. The noncollinearity of the moments (lower panel) leads to the narrowing of the bands and to the mixing and hybridizational repulsion of the states with opposite spin projections. See the text of the paper for the discussion of the relation between these changes and exchange interactions.

Summarizing the properties of the DOS we conclude that all systems studied are either half-metallic (the charge carriers are in one spin-channel only) or insulating (no charge carriers). This is a consequence of the position of, at least, a part of the $3d$ impurity bands within the wide semiconducting gap of ZnO.

To reveal the relations between electronic structure and effective interatomic exchange interactions in a magnetic system is one of the important tasks of the theory of magnetism. Most of the models of the exchange interactions in DMS assume a decisive role of the charge carriers in establishing long-range ferromagnetic order. For example, the Zener model is applied to study the mediation of the magnetism by the sp states of the semiconductor matrix.¹ On the other hand, the double-exchange model is based on a physical picture of the d electron hopping between atoms with strong on-site Hund's exchange.¹⁵ In the DMS systems studied in this paper, the states of the partially filled energy bands have a high $3d$ contribution and therefore the double-exchange picture is more appropriate.

In contrast to the carrier-mediated ferromagnetism, the exchange through completely filled bands is expected to lead to an antiferromagnetic interatomic exchange interaction.¹⁶

The parameters of the effective exchange interactions calculated within the frozen-magnon approach reflect the energy price of the deviation of the atomic moments from the parallel directions. An energy increase with the deviation reveals the stability of the ferromagnetic state. The larger the increase, the larger the exchange interactions and, as a result, the Curie temperature. On the other hand, the decrease of the energy with the deviation from parallel directions means instability of the ferromagnetism and an antiferromagnetic character of the exchange interactions.

In Fig. 4 two physical mechanisms leading to ferromagnetic and antiferromagnetic types of exchange interactions are illustrated schematically in the form they appear in the density-functional-theory calculations. The ferromagnetic state of a model system is characterized by two energy bands

of opposite spin projections. There are two kinds of changes in the electronic structure that arise with the deviation of the atomic moments from the parallel directions. The first kind bears some features of the double-exchange mechanism and consists in the narrowing of the bands. The presence of the narrowing can, for example, be shown within a tight-binding model of a frozen-magnon state.^{10,19}

The band narrowing can be interpreted as an increase of the effective mass of an electron moving in the exchange field produced by a noncollinear configuration of the atomic exchange fields. If the band is partially filled, the narrowing leads to an increase of the total energy. The larger the band width of the unperturbed ferromagnet, the larger the energy increase resulting from the narrowing.

The second effect caused by the noncollinearity is the hybridization between the majority and minority spin states. Indeed, in a collinear ferromagnet the spin projection of the electron states is a good quantum number and, therefore, the bands with the opposite projections do not mix. The noncollinearity destroys the spin projection as a good quantum number leading to the spin mixing of the states. In the model considered in Fig. 4 this mixing leads to the hybridizational repulsion of the subbands resulting in a lower energy position of the lower subband and a higher energy position of the upper subband. The consequence of this process is the decrease of the energy of the system. This decrease is maximal in the case when the lower band is completely filled and the upper band is empty. Since for a completely filled band the double-exchange effect is absent, the leading exchange mechanism is in this case antiferromagnetic. The strength of the hybridizational repulsion is reverse proportional to the energy distance between the interacting states: the closer the interacting bands, the stronger the effect.

Although the schematic picture presented in Fig. 4 strongly simplifies the actual processes taking place in a realistic many-band system, it is useful for the qualitative interpretation of the calculated exchange interactions reported below.

C. Calculated exchange interactions

In Fig. 5 we present calculated exchange parameters. The strength of the exchange interaction decays quickly with increasing distance between interacting atoms. As a result, only the nearest-neighbor interactions are important. The interactions are much stronger in the case of high impurity concentrations, which agrees with our qualitative picture of the relation between the band widths and the strength of the exchange interactions.

The sign of the leading exchange interaction is different for different DMS. In (ZnMn)O, the interaction is antiferromagnetic for both impurity concentrations. The antiferromagnetic interaction is very strong for the concentration of 25%. Since for both concentrations the majority-spin subband is completely filled and the minority-spin subband is empty, the antiferromagnetic type of the exchange interaction is expected.

In the Co system we obtain the transition from a ferromagnetic interaction for the high impurity concentration to

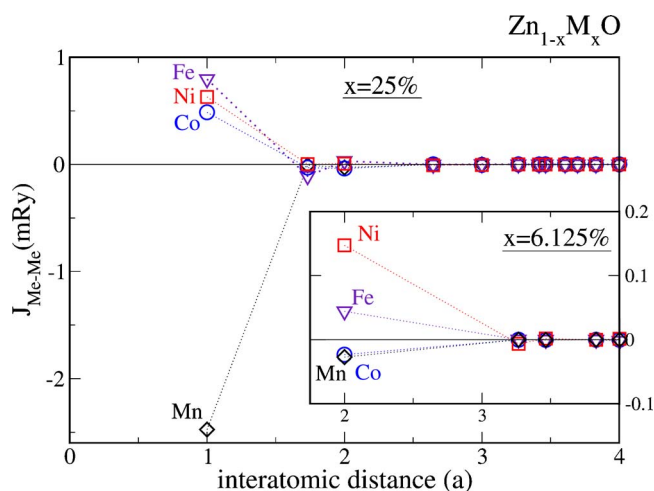


FIG. 5. (Color online) Calculated exchange parameters (ZnMe)O for the impurity concentration of 25% and 6% (inset).

an antiferromagnetic interaction for the low one. This transition can be explained on the basis of the properties of the DOS. Indeed, the crystal field splitting of the minority $3d$ states leads to the separation of two groups of the states. Since the lower group is completely filled and the upper one is empty, the analysis of Fig. 4 can be applied to explain the negative sign of the exchange interaction. In this case the hybridizational repulsion can take place between the filled minority-spin impurity band and empty majority-spin states of the conduction band as well as between the filled states of the majority-spin impurity band and the states of the empty minority-spin impurity subband. These interactions are weak resulting in small values of exchange parameters.

In the case of (ZnFe)O and (ZnNi)O the leading interactions are ferromagnetic for both impurity concentrations assuming larger values for larger concentrations.

D. Curie temperature

The calculated exchange parameters are used to estimate the Curie temperature. To gain a deeper insight into the magnetic properties of the systems we estimate the Curie temperature for different numbers of valence electrons. The variation of the electron number in a real sample can be caused by the presence of additional nonmagnetic donors or acceptors. In Figs. 6 and 7 the nominal number of electrons corresponds to $n=0$. The negative values of the Curie temperature correspond to the antiferromagnetic leading exchange interaction and reflect the instability of the ferromagnetism in the ground state.

We observe that in the cases where the nominal electron number corresponds to the absence of the charge carriers [(ZnMn)O for both concentrations and (ZnCo)O for low concentration], the value of $n=0$ gives a minimum of the exchange interaction. Here, the deviation from $n=0$ to either positive or negative directions creates carriers and leads to an increasing ferromagnetic contribution to the exchange parameters.

For $x=25\%$, the highest Curie temperature at the nominal electron number is obtained for (ZnFe)O (453 K) followed

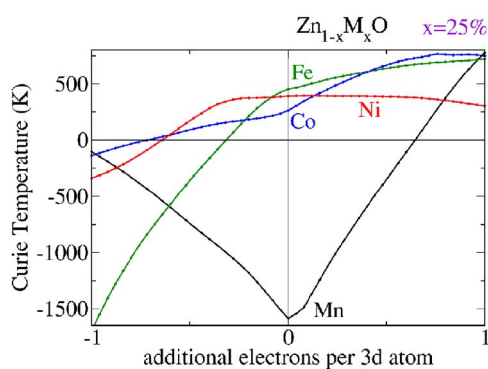


FIG. 6. (Color online) Calculated Curie temperatures (ZnMe)O for the impurity concentration of 25%. The negative values of the Curie temperature reveal instability of the ferromagnetic configuration in the ground state.

by (ZnNi)O (389 K) and (ZnCo)O (262 K). On the other hand, (ZnCo)O shows strong potential to increasing Curie temperature with increasing electron number.

For $x=6.25\%$ the highest T_c is obtained for (ZnNi)O (93 K) followed by (ZnFe)O (27 K). In this case, the variation of the electron number does not lead to an increase of the Curie temperature.

III. CONCLUSIONS

We have studied the electronic structure and exchange interactions in four DMS semiconductors on the ZnO basis for two impurity concentrations of 25% and 6.25%. For all systems, the interatomic exchange interactions are short range with only the interaction between the nearest $3d$ impurities being sizable. For (ZnMn)O, the leading exchange interaction is antiferromagnetic for both impurity concentrations. In (ZnCo)O, the leading exchange interaction is ferromagnetic for high concentration and antiferromagnetic for low concentration. (ZnFe)O and (ZnNi)O are ferromagnetic for both concentrations. In all cases of the antiferromagnetic exchange interaction, the energy bands are either completely filled or empty. This reveals the connection between the presence of the charge carriers and ferromagnetism.

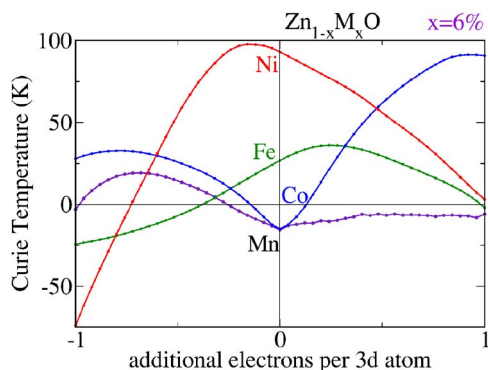


FIG. 7. (Color online) The same as in Fig. 6 but for impurity concentration of 6%.

At $x=25\%$, the highest estimation of the Curie temperature for a nominal electron number is obtained for (ZnFe)O and assumes the value of 453 K. (ZnCo)O shows high potential for the increase of the Curie temperature with increasing number of electrons. At $x=6.25\%$, the highest Curie temperature for nominal electron number is obtained for (ZnNi)O. For this concentration we do not obtain strong potential for an increase of T_c with the variation of the electron number for either of the materials.

We conclude the paper with a number of comments on some aspects and desired extensions of this work. First, we do not compare our calculational data with experiment. By the present strong scattering of the experimental information on the character of the magnetic ground state, such a comparison is not informative. The purpose of this paper is to stimulate further experimental studies by providing new theoretical information.

Second, an important issue in the physics of the systems containing $3d$ atoms is the on-site Coulomb correlations. There are several theoretical schemes allowing the treatment of these correlations beyond LDA. One of the popular approaches is the so-called LDA+ U method.²⁰ It is certainly of

strong interest to perform the calculations reported here within the LDA+ U scheme. Our previous studies of the DMS systems with the use of both LDA and LDA+ U approaches have shown that the use of Hubbard U can lead to both increase and decrease of the magnetic transition temperature.²¹ Depending on the system, some features of the electronic structure can show surprising stability with respect to the calculational approach.²² In the recent letter on (GaMn)As, Xu *et al.*²³ reported good quantitative agreement between experimental Curie temperatures and the theoretical values obtained within LDA. In other cases the LDA+ U scheme seems to be more appropriate.¹¹ Concerning the results discussed in the given paper we expect that the connection between the presence of partially filled bands and the ferromagnetism will be preserved also in the LDA+ U calculations. The values of the exchange parameters and magnetic transition temperatures can change substantially.

Third, in the present calculation we did not consider the structural relaxation about the impurities. On the basis of our previous experiences we do not expect a strong influence of the relaxation on the exchange interactions.²⁴ The direct calculations are desirable.

¹T. Dietl, H. Ohno, F. Matsukura, J. Cibert, and D. Ferrand, *Science* **287**, 1019 (2000).

²K. Ueda, H. Tabata, and T. Kawai, *Appl. Phys. Lett.* **79**, 988 (2001); K. Ando, H. Saito, Zhengwu Jin, T. Fukumura, M. Kawasaki, Y. Matsumoto, and H. Koinuma, *ibid.* **78**, 2700 (2001); T. Fukumura, Z. W. Jin, M. Kawasaki, T. Shono, T. Hasegawa, S. Koshihara, and H. Koinuma, *ibid.* **78**, 958 (2001); S. W. Jung, S.-J. An, G.-C. Yi, C. U. Jung, S.-I. Lee, and S. Cho, *ibid.* **80**, 4561 (2002); Y. M. Cho, W. K. Choo, H. Kim, D. Kim, and Y. E. Ihm, *ibid.* **80**, 3358 (2002); W. Prellier, A. Fouchet, B. Mercey, Ch. Simon, and B. Raveau, *ibid.* **82**, 3490 (2003); D. P. Norton, M. E. Overberg, S. J. Pearton, K. Pruessner, J. D. Budai, L. A. Boatner, M. F. Chisholm, J. S. Lee, Z. G. Khim, Y. D. Park, and R. G. Wilson, *ibid.* **83**, 5488 (2003); K. Rode, A. Anane, R. Mattana, J.-P. Contour, O. Durand, and R. LeBourgeois, *J. Appl. Phys.* **93**, 7676 (2003); Y. W. Heo, M. P. Ivill, K. Ip, D. P. Norton, S. J. Pearton, J. G. Kelly, R. Rairigh, A. F. Hebard, and T. Steiner, *Appl. Phys. Lett.* **84**, 2292 (2004); S. Ramachandran, A. Tiwari, and J. Narayan, *ibid.* **84**, 5255 (2004); M. Venkatesan, C. B. Fitzgerald, J. G. Lunney, and J. M. D. Coey, *Phys. Rev. Lett.* **93**, 177206 (2004).

³R. Janisch, P. Gopal, and N. A. Spaldin, *J. Phys.: Condens. Matter* **17**, R657 (2005).

⁴K. Sato and H. Katayama-Yoshida, *Jpn. J. Appl. Phys., Part 2* **40**, L334 (2001).

⁵E. Kulatov, Y. Uspenskii, H. Mariette, J. Cibert, D. Ferrand, H. Nakayama, and H. Ohta, *J. Supercond.* **16**, 123 (2003).

⁶A. S. Risbud, N. A. Spaldin, Z. Q. Chen, S. Stemmer, and R. Seshadri, *Phys. Rev. B* **68**, 205202 (2003).

⁷N. A. Spaldin, *Phys. Rev. B* **69**, 125201 (2004).

⁸M. S. Park and B. I. Min, *Phys. Rev. B* **68**, 224436 (2003).

⁹L. M. Sandratskii and P. Bruno, *Phys. Rev. B* **66**, 134435 (2002).

¹⁰L. M. Sandratskii and P. Bruno, *Phys. Rev. B* **67**, 214402 (2003).

¹¹L. M. Sandratskii, *Phys. Rev. B* **68**, 224432 (2003).

¹²A. R. Williams, J. Kübler, and C. D. Gelatt, *Phys. Rev. B* **19**, 6094 (1979).

¹³D. Vogel, P. Krüger, and J. Pollmann, *Phys. Rev. B* **54**, 5495 (1996).

¹⁴It is worth making a comment on the application of the Hund's rule to the analysis of the condensed-matter systems. This rule is formulated for an isolated atom. The interatomic hybridization present in the condensed-matter systems can strongly weaken the trends produced by the Hund's rule. For instance, the ground state of the bulk vanadium is nonmagnetic while the Hund's rule predicts for a V atom the spin moment $S=3/2$. In the case of the $3d$ impurities in ZnO, our calculations show that the trends originating from the Hund's rule are still well observed.

¹⁵P. M. Krstajic, F. M. Peeters, A. Ivanov, V. Fleurov, and K. Kikoin, *Phys. Rev. B* **70**, 195215 (2004).

¹⁶The actual situation is more complex. The Anderson's expression for the antiferromagnetic superexchange parameter $J=-b^2/\delta$ is obtained under simplified assumptions.¹⁷ In its essence, this is a standard second-order perturbation expression for the energy of a nondegenerate level where δ is the energy distance to the first excited state and b is a small parameter describing the efficiency of the interlevel interaction caused by the perturbation. The consideration of more realistic multiple-orbital models, the concrete structural geometry, higher order perturbation effects can lead to ferromagnetic character of the superexchange (see, e.g.,^{17,18}). In this paper we do not use a model Hamiltonian to evaluate the exchange parameter. Instead, the parameter-free density-functional-theory (DFT) calculations are employed. The parallel with the model Hamiltonian considerations is, however, useful. In Fig. 4, we present two mechanisms contributing to the exchange interactions within the DFT picture. These mechanisms by no means exhaust the variety of contributions to the exchange interactions that can play important role in the complex multiple-band materials. However, for the DMS systems consid-

- ered in the paper, the two mechanisms presented allow a qualitative interpretation of the relation between the calculated exchange parameters and the electronic structure.
- ¹⁷P. W. Anderson, Phys. Rev. **115**, 2 (1959).
- ¹⁸J. B. Goodenough, Phys. Rev. **100**, 564 (1955); P. Kacman, Semicond. Sci. Technol. **16**, R25 (2001).
- ¹⁹L. M. Sandratskii and P. Bruno, *Local Moment Ferromagnets: Unique Properties for Modern Applications*, edited by M. Donath and W. Nolting (Springer, New York, 2005).
- ²⁰V. I. Anisimov, F. Aryasetiawan, and A. I. Lichtenstein, J. Phys.: Condens. Matter **9**, 767 (1997).
- ²¹L. M. Sandratskii, P. Bruno, and J. Kudrnovský, Phys. Rev. B **69**, 195203 (2004).
- ²²A. Ernst, L. M. Sandratskii, M. Bouhassone, J. Henk, and M. Lüders, Phys. Rev. Lett. **95**, 237207 (2005).
- ²³J. L. Xu, M. van Schilfgaarde, and G. D. Samolyuk, Phys. Rev. Lett. **94**, 097201 (2005).
- ²⁴L. M. Sandratskii, P. Bruno, and S. Mirbt, Phys. Rev. B **71**, 045210 (2005).